2-2014

Investigation of Profiled Beam Propagation through a Turbulent Layer and Temporal Statistics of Diffracted Output for a Modified von Karman phase Screen

Monish Ranjan Chatterjee
University of Dayton, mchatterjee1@udayton.edu

Fathi H.A. Mohamed
University of Dayton

Investigation of Profiled Beam Propagation through a Turbulent Layer and Temporal Statistics of Diffracted Output for a Modified von Karman Phase Screen

Monish R. Chatterjee[1,*] and Fathi H. A. Mohamed[1]

[1]Department of Electrical & Computer Engineering

University of Dayton, Dayton, Ohio 45469

[*]Corresponding author

ABSTRACT

Gaussian beam propagation through a turbulent layer has been studied using a split-step methodology. A modified von Karman spectrum (MVKS) model is used to describe the random behavior of the turbulent media. Accordingly, the beam is alternately propagated (i) through a thin Fresnel layer, and hence subjected to diffraction; and (ii) across a thin modified von Karman phase screen which is generated using the power spectral density (PSD) of the random phase obtained via the corresponding PSD of the medium refractive index for MVKS turbulence. The random phase screen in the transverse plane is generated from the phase PSD by incorporating (Gaussian) random numbers representing phase noise. In this paper, numerical simulation results are presented using a single phase screen whereby the phase screen is located at an arbitrary position along the propagation path. Specifically, we examine the propagated Gaussian beam in terms of several parameters: turbulence strength, beam waist, propagation distance, and the incremental distance for Fresnel diffraction for the case of extended turbulence. Finally, on-axis temporal statistics (such as the mean and variance) of the amplitude and phase of the propagated field are also derived.

Keywords: Atmospheric turbulence**,** Gaussian beam, Modified von Karman spectrum, split-step beam propagation method, random phase screen.

1. INTRODUCTION

Atmospheric turbulence effects may have a strong influence on several laser applications whereby the turbulence causes fluctuations in both the intensity and the phase of the received light signal. Experimental studies of atmospheric turbulence effects on laser beam propagation is of importance in relating environmental parameters to beam propagation effects and estimate magnitudes of perturbations which degrade the performance of laser systems [1]. Theoretical descriptions in the intermediate and strong turbulence regimes are less well developed than for weak turbulence. Knowledge of atmospheric turbulence effects is helpful in the development of a wide class of atmospheric-optics systems including laser communication, energy transfer, remote sensing, and active and passive imaging systems. Inhomogeneities in the temperature and pressure of the atmosphere lead to variations of the refractive index along the transmission path. Index inhomogeneities can deteriorate the quality of the received signal and cause fluctuations in both the intensity and the phase of the received signal. Several atmospheric turbulence spectral models use random phase screens to model the turbulence [2-5]. Common among these are the Kolmogorov, Tatarski, von Karman and modified von Karman spectra (MVKS). The phase fluctuations of the phase screen used to model the random phase distribution within the aperture are parameterized by the Fried parameter, which describes the transverse coherence length, and the inner and outer scales that determine the amount of aberration seen by the propagating beam. The split-step propagation method involving the Fresnel-Kirchhoff diffraction integral is used to model the propagation of the

Free-Space Laser Communication and Atmospheric Propagation XXVI, edited by Hamid Hemmati, Don M. Boroson,
Proc. of SPIE Vol. 8971, 897102 · © 2014 SPIE · CCC code: 0277-786X/14/$18 · doi: 10.1117/12.2033442

electromagnetic wave through turbulence media wherefrom the scintillation index (SI) and fringe visibility (FV) may be calculated [3].

Modeling laser beam propagation through turbulence using successive phase screens provides an efficient tool for tracking the effect of atmospheric turbulence laser beam propagation. In this work, a split-step beam propagation method (SSBPM) is used whereby either a single random phase screen or extended (multiple) random phase screens are placed at arbitrary location(s) along the propagation path. In addition, the PSD of the MVKS spectrum is used in this work due to its simplicity while still including both the inner and outer scales defining the inertial range for turbulent eddies.

In this paper, we have studied the effect of atmospheric turbulence on the propagation of a Gaussian beam profile. This study was prompted by the eventual desire to propagate a modulated chaotic wave generated from an acousto-optic cell with feedback through the turbulence. In the initial stages of the work, two scenarios were followed: (a) a single random phase screen located at a specific distance from the aperture plane for which the field intensity at the observation (image) plane is numerically calculated, and (b) extended (multiple) random phase screens that are placed an infinitesimal distance (Δz) apart and once again the field intensity at different positions and at the image plane is calculated using the split-step algorithm. Three parameters were chosen for both cases: (a) strength of turbulence (weak or strong), (b) width of the profiled Gaussian beam (with beam waist w_0 either wide or narrow), and (c) propagation distance L. More details about theses parameters will be discussed with the simulation results and interpretation. We also note that in this paper, we only report the results for a single planar phase screen placed along the propagation path. Also, some work regarding *on-axis* time statistics of diffracted amplitude and phase in the image plane during propagation in atmospheric turbulence is discussed for the case of a *thin* turbulent layer represented by a planar random phase screen.

The outline of this paper is as follows. In section 2, the split-step propagation method incorporating the Fresnel-Kirchhoff diffraction integral is discussed briefly. A general overview of the turbulence, its models and random phase screen generation is presented in section 3. The simulation results and interpretations are reported in some detail in section 4. Section 5 provides concluding remarks and an outline of ongoing and future work.

2. THE SPLIT-STEP BEAM PROPAGATION METHOD

Most atmospheric turbulence simulations use the split-step algorithm to mimic the turbulence and it is a common method for the analysis of laser beam propagation through inhomogeneous media. In this paper, we have applied the SSBPM to all numerical simulations for single and multiple phase screens and for time-statistical analyses of atmospheric turbulence. We introduce here a brief description of SSBPM. It is known that the beam propagation method is used widely for the numerical simulation of propagation through inhomogeneous, anisotropic, and nonlinear materials including waveguiding structures with weak variations along the propagation direction [9]. The method relies on computing the solutions in infinitesimally small steps taking into account the linear and nonlinear (or non-deterministic) steps separately.

The key methodology behind the SSBPM are two-fold. First, the expected propagation distance is sectioned into infinitesimal segments. Secondly, the linear processes (such as diffractive integrals) are performed between the spatial frequency domain or k-space and the spatial coordinates, which are interrelated. Correspondingly, the random phase function defined by the MVKS model ($\Phi_n(k)$) is in the spatial frequency domain as such; it is then processed via a series of transformations so that we finally obtain a spatial phase distribution φ_{ij}, where the subscripts (i,j) imply spatial coordinates of points on the chosen grid within which the phase distribution is applied. In the case of extended turbulence (with multiple random phase screens), not reported here, the propagation distance, L, is divided into increments $\Delta z = L/n$, where n is the number of random phase screens [10].

In the SSBPM, we begin with the profiled electromagnetic (EM) beam at z = 0. The profiled beam (Gaussian in our case) travels the first longitudinal increment (Δz) (from z to z + Δz). In this distance (Δz), the field is subjected to the familiar Fresnel-Kirchhoff diffraction integral with z replaced by Δz as follows:

$$U(x_i, y_i) = \iint_{-\infty}^{\infty} U(x_o, y_o) e^{\left\{j\frac{k}{2z}[(x_i - x_o)^2 + (y_i - y_o)^2]\right\}} \, dx_o dy_o \,, \tag{1}$$

where $U(x_o, y_o)$ is the input profiled beam, $U(x_i, y_i)$ is the field after distance Δz, k is the unbounded wave number and λ is the wavelength in the medium.

When the profiled EM wave reaches the first random phase screen, the second operator in the algorithm describes the effect of propagation in the absence of diffraction and in the presence of the medium inhomogeneities (random phase screen in our case); this is incorporated in the spatial domain. Hence, after a distance of Δz, the phase perturbations caused by refractive index fluctuation arising from turbulence effects are represented by multiplying the field by a phase function $e^{j\varphi(x,y)}$ as:

$$U_{out}(x_i, y_i) = U_{in}(x_i, y_i)\, e^{j\varphi(x_i, y_i)} \quad , \tag{2}$$

where $U_{out}(x_i, y_i)$ is the field amplitude immediately after random phase screen, and $U_{in}(x_i, y_i)$ is the field before random phase screen. The above process is repeated until the field has traveled the desired distance.

All the simulation results presented in this paper were carried out using SSBPM. In the case of a single phase screen, the propagation path is divided into two segments: (a) from the input profiled Gaussian beam to the phase screen, and (b) from the phase screen to the observation plane at z = L. The single phase screen may be considered as a special case of the extended phase screen. For the extended phase screen (representing a wide range of turbulence), it is found that a tradeoff is needed between the accuracy and complexity. Thus, for a given propagation distance, if the number of phase screens is increased, the corresponding incremental diffractive distance (Δz) will be lower. This leads to an increase in the processing time. Ideally, for better representation of the atmospheric turbulence over an extended medium, one must use the conditions Δz→0 and number of phase screens → ∞.

3. ATMOSHERIC TURBULENCE

In this section, we briefly introduce a brief overview of atmospheric turbulence and in particular the modified von Karman (MVKS) phase turbulence model. We also discuss numerical generation of the random phase screen which describes the random behavior of the turbulence over a thin transverse layer in the propagation direction. The characteristics of the optical wave transmitted through atmospheric turbulence can undergo dramatic changes resulting in potential system performance degradation. In standard turbulence modeling, three parameters characterizing atmospheric turbulence play an important role in describing medium behavior: the refractive index structure parameter (C_n^2) which describes the strength of the atmospheric turbulence, and the inner (l_0), and outer (L_0) scales of turbulence eddies. The work reported here is a part of ongoing research involving propagation of chaotic (and encrypted) EM waves through atmospheric turbulence.

3.1 von Karman Spectrum

The power spectrum density of the von Karman Spectrum (also called the modified von Karman spectrum (MVKS) in the form shown) is given by [11]:

$$\Phi_n(k) = 0.033\, C_n^2 \, \frac{\exp\left(-\frac{k^2}{k_m^2}\right)}{\left(k^2 + k_0^2\right)^{\frac{11}{6}}} \quad , \; 0 \leq k \ll \infty \tag{3}$$

where C_n^2 is the medium structure parameter, $k_m = {}^{5.92}/_{l_o}$ is an equivalent wavenumber related to the inner scale, $k_{m0} = {}^{2\pi}/_{L_o}$ is a wavenumber related to the outer scale, and k is the unbounded non-turbulent wavenumber in the medium. In the above equation, $\Phi_n(k)$ represents the so-called power spectral density (PSD) of the refractive index of the medium.

3.2 Thin phase screen generation

In this section we discuss the generation of a phase screen to mimic the statistical behavior of the phase fluctuations due to a turbulent atmosphere using a discrete grid and generating the phase screen from the given spectrum based on fast Fourier transform (FFT) techniques. The purpose of a phase screen is to simulate the random phase perturbations resulting from random index fluctuations in extended atmospheric turbulence [12]. The generated random phase screen (either planar or extended) in this paper is characterized by several different parameters: C_n^2 (or Fried parameter r_0), inner and outer scales, l_0 and L_0 respectively, and the incremental spatial frequencies $\Delta k_x,\ \Delta k_y$.

The procedure of phase screen generation is as follows: beginning with the MVKS model with given parameters as mentioned, and by using a standard scheme based on Fourier transform generation, a set of random complex numbers (following a Gaussian distribution) is generated on the chosen grid. Following eq. (4), the random numbers are multiplied by the square root of the phase power spectrum (PPS) wherefrom an inverse Fourier transform produces the phase screen. The real part of the result is taken to be the random phase function $\varphi(x, y)$ due to atmospheric fluctuations based on the MVKS model. The discrete phase distribution in 2-D is given as:

$$\varphi_{ij} = Re\{IFFT((a+ib)\sqrt{\Phi_p \Delta k_x \Delta k_y})\}\ , \tag{4}$$

where *IFFT* represents the inverse *fast Fourier transform* operation, Φ_p is the power spectral density (given below) evaluated in the transverse plane, and a and b are random numbers generated in order to appropriately mimic the random noise-like characteristics of the von Karman phase. The MVKS power spectral density may be expressed as:

$$\Phi_p(k) = 0.23\, r_0^{-\frac{5}{3}} \frac{\exp\left(-\frac{k^2}{k_m^2}\right)}{\left(k^2+k_o^2\right)^{\frac{11}{6}}} \quad . \tag{5}$$

4. NUMERICAL SIMULATIONS, RESULTS, AND INTERPRETATIONS

In this section, we present numerical simulation results of the profiled Gaussian beam passing through turbulence medium. In this paper, we present results for a planar random phase screen placed at a pre-determined location along the propagation. We also report some time statistics corresponding to the diffracted field amplitude and phase on axis at the image plane. Some of the parameters are kept constant during the simulation process. These parameters consist of: number of sample points (grid resolution) = 512x512, wavelength λ=1μm, physical size of grid = 500mmx500mm, inner scale $l_0 = 10\text{mm}$, and outer scale $L_0 = 3000\text{mm}$ respectively. As we mentioned earlier, the other parameters (C_n^2 or r_0, w_0, and L) are varied depending on weak or strong turbulence, wide or narrow Gaussian beam, and different propagation path lengths. For an extended phase screen we also have the longitudinal increment (Δz), which is the physical distance between two successive phase screens.

4.1 Single phase screen

In the following, we place the random phase screen at the locations 0, 0.5L, and L. A Gaussian beam is then propagated first from the object plane to the phase screen under near-field condition, and thereafter, following passage through the screen, once again via the diffraction integral to the image plane. The resulting beam profile, phase distribution and the scalar field amplitudes are then determined at the image plane.

Case I. Turbulence strength

In standard atmospheric turbulence literature, it is known that the numerical ranges of the structure parameter C_n^2 defining strong, intermediate and weak turbulence are defined as:

$C_n^2 > 10^{-14}$ m-2/3	strong
$10^{-16} < C_n^2 < 10^{-14}$ m-2/3	intermediate
$C_n^2 < 10^{-17}$ $m^{-2/3}$	*weak*

While the above represents the necessary values of the structure parameter defining a certain turbulence regime, we also need to specify the so-called Fried parameter r_0 corresponding to the chosen C_n^2. This is obtained via the relation:

$$r_0 = 0.185\left[\frac{4\pi^2}{k^2\, L\, C_n^2}\right]^{3/5}, \tag{6}$$

where k is the unbounded wave number, and L is the propagation distance.

(a) Weak turbulence

Using the above information, one may arrive at a weak turbulence regime defined by:

r_0=10 mm or C_n^2=1.067x10^{-18} m$^{-2/3}$.

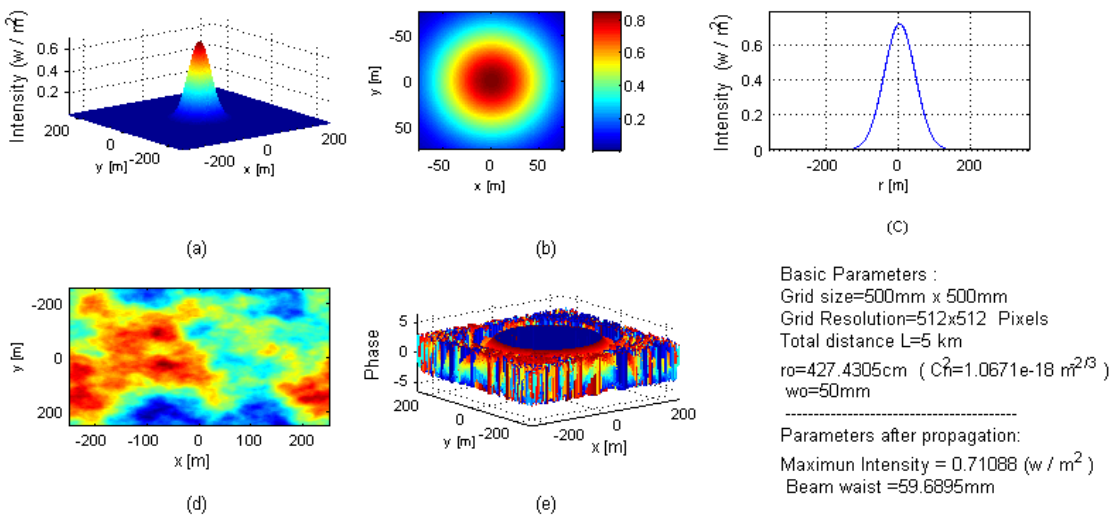

Fig.1. Gaussian beam propagation to distance z=L (phase screen at the object plane). (a) 3-D Gaussian beam, (b) Gaussian beam cross-section, (c) Gaussian beam profile, (d) Random phase screen profile, and (e) Gaussian beam phase distribution in transverse output plane.

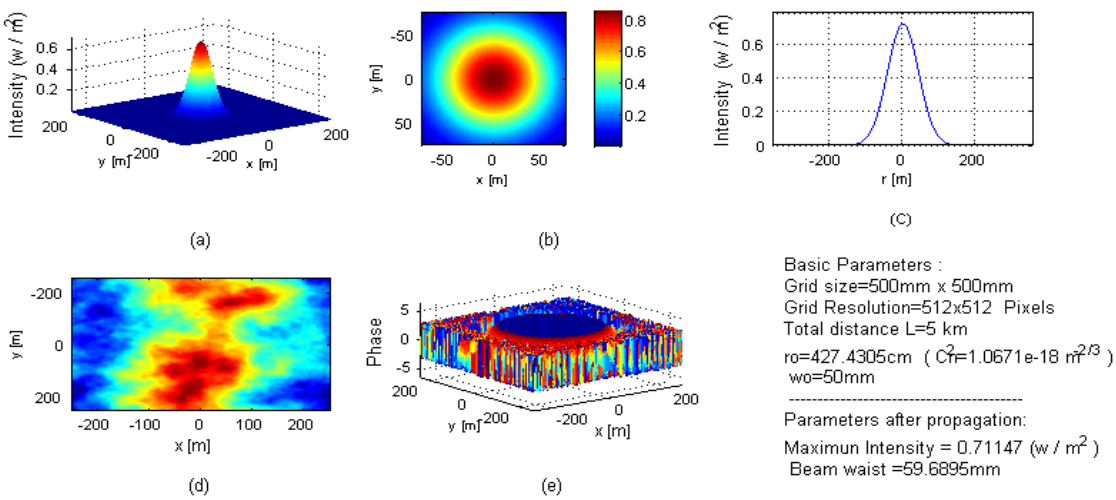

Fig.2. Gaussian beam propagation to distance z=L (phase screen at .5L). (a) 3-D Gaussian beam, (b) Gaussian beam cross-section, (c) Gaussian beam profile, (d) Random phase screen profile, and (e) Gaussian beam phase distribution in transverse output plane.

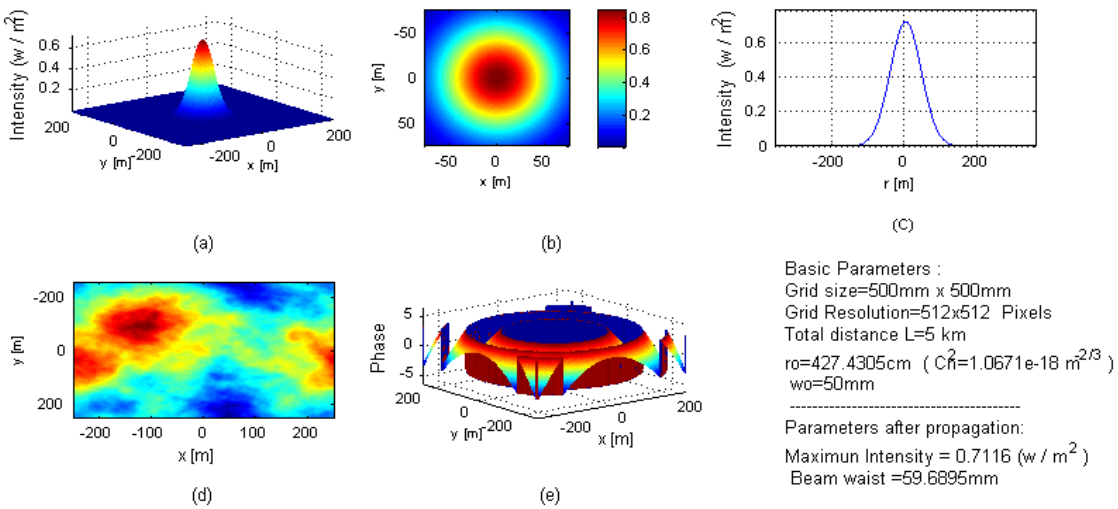

Fig.3. Gaussian beam propagation to distance z=L (phase screen at L or image plane). (a) 3-D Gaussian beam, (b) Gaussian beam cross-section, (c) Gaussian beam profile, (d) Random phase screen profile, and (e) Gaussian beam phase distribution in transverse output plane.

(b) Strong turbulence

Similarly, for this case, we choose r_0=0.01mm or C_n^2=1.067x10^{-13} m$^{-2/3}$.

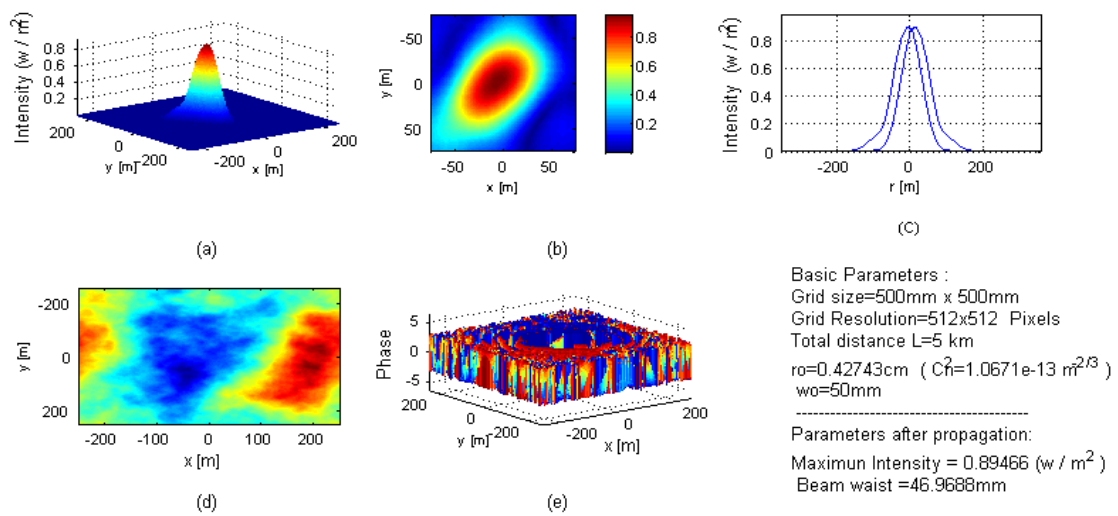

Fig.4. Gaussian beam propagation to distance z=L (phase screen at the object plane). (a) 3-D Gaussian beam, (b) Gaussian beam cross-section, (c) Gaussian beam profile, (d) Random phase screen profile, and (e) Gaussian beam phase distribution in transverse output plane.

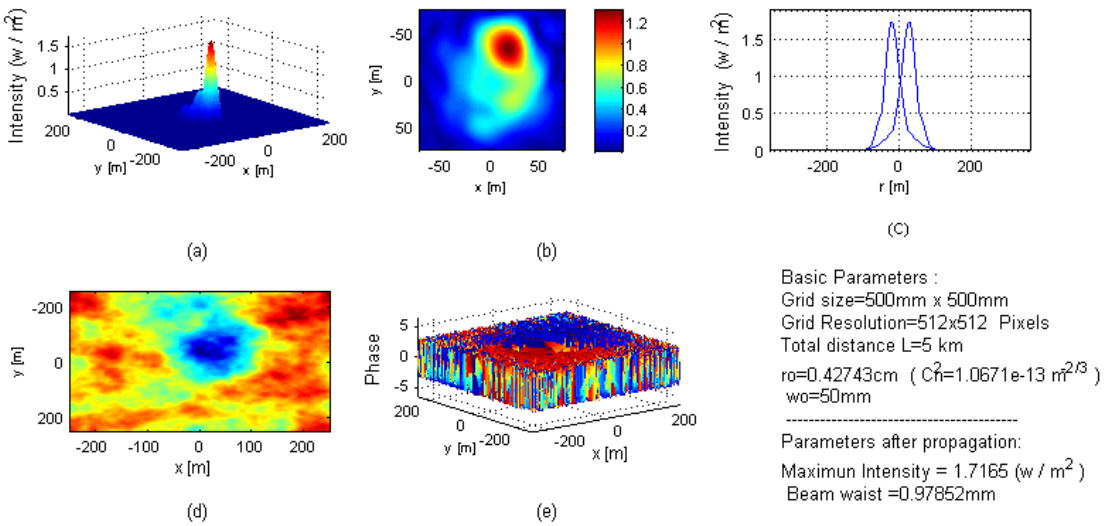

Fig.5. Gaussian beam propagation to distance z=L (phase screen at .5L). (a) 3-D Gaussian beam, (b) Gaussian beam cross-section, (c) Gaussian beam profile, (d) Random phase screen profile, and (e) Gaussian beam phase distribution in transverse output plane.

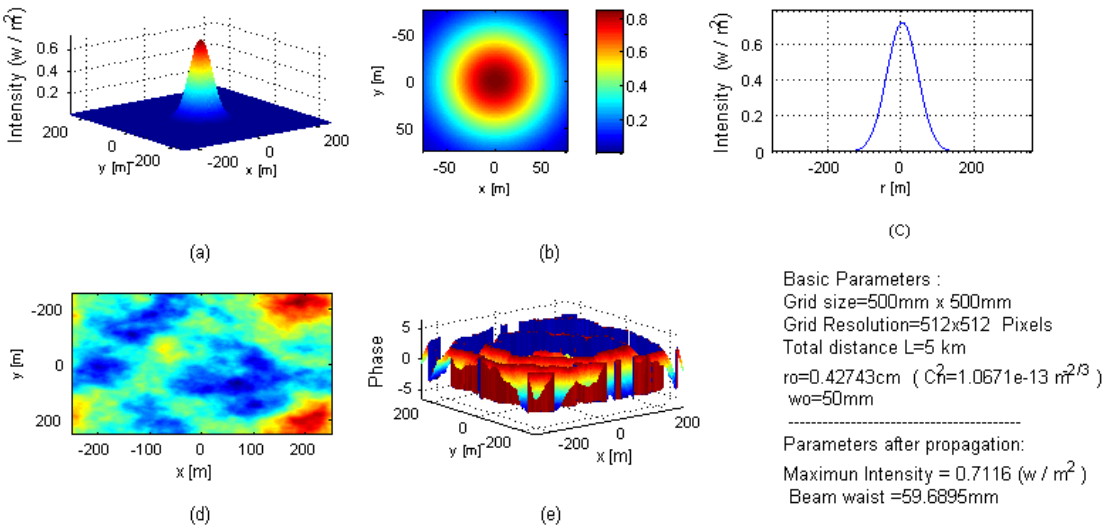

Fig.6. Gaussian beam propagation to distance z=L (phase screen at L or image plane). (a) 3-D Gaussian beam, (b) Gaussian beam cross-section, (c) Gaussian beam profile, (d) Random phase screen profile, and (e) Gaussian beam phase distribution in transverse output plane.

From Figs. 1-6, we observe that the Gaussian beam suffers more amplitude distortion and likely more phase fluctuations for strong turbulence compared to weak turbulence. Regarding the random phase screen placement, we find that the phase fluctuations increase when the phase screen is placed at the beginning of the propagation distance (at 0) or the middle (0.5L) compared to the end (L) relative to the propagation path. An intuitive interpretation might be as follows. Thus, when the phase screen is placed at 0, the propagated beam passes through the random phase screen (turbulence) before any kind of self-diffraction along the propagation path, while when the phase screen at the image plane (at z=L), the propagated beam is subjected to self-diffraction before it reaches the random phase screen at the end. In other words, when an EM beam acquires a random phase profile, the resulting phase fluctuations are more

pronounced as the beam propagates over an arbitrary distance under self-diffraction. On the other hand, when the beam initially self-diffracts with a deterministic phase profile, and encounters a random phase at the end, the exiting beam does not experience a comparable rate of phase fluctuations. We may also note that under weak turbulence, while the phase fluctuations may still be pronounced, the amplitude or intensity profile remains relatively unaffected. Also, under weak turbulence, the incident Gaussian undergoes peak amplitude (or intensity) decay during propagation. Since the medium is considered lossless, this decay simply implies a lowering of the Gaussian peak as the profile broadens due to diffraction. Under strong turbulence, on the other hand, for earlier screen placement, the diffracted beam not only splits and consequently distorts, it also experiences apparent peak intensity increase. This might seem to be contradictory for a lossless propagation; however, we note that the increased intensity peak is probably misleading, and more likely there occurs split output amplitudes of opposite polarities that would still conserve net energy and power. Since the plots show intensity (which is amplitude-squared), this feature is not visible in the plots. Further quantitative analyses to affirm these findings are pending.

Case II. Waist of the Gaussian beam

In this case, we consider moderate turbulence ($r_0 = 0.5$ mm, or $C_n^2 = 1.5725 \times 10^{-16}$ $m^{-2/3}$).

We consider also the physical size of the Gaussian beam, which we define in the following as narrow or wide. In this series, both narrow and wide will imply Gaussian beams whose spot size ($2w_0$) fits well within the size of the diffraction grid. Thus, narrow and wide beams are only defined in terms of the relative spot sizes of the beams, and not necessarily in terms of comparison with the aperture.

(a) Narrow Gaussian beam (w0=10 mm)

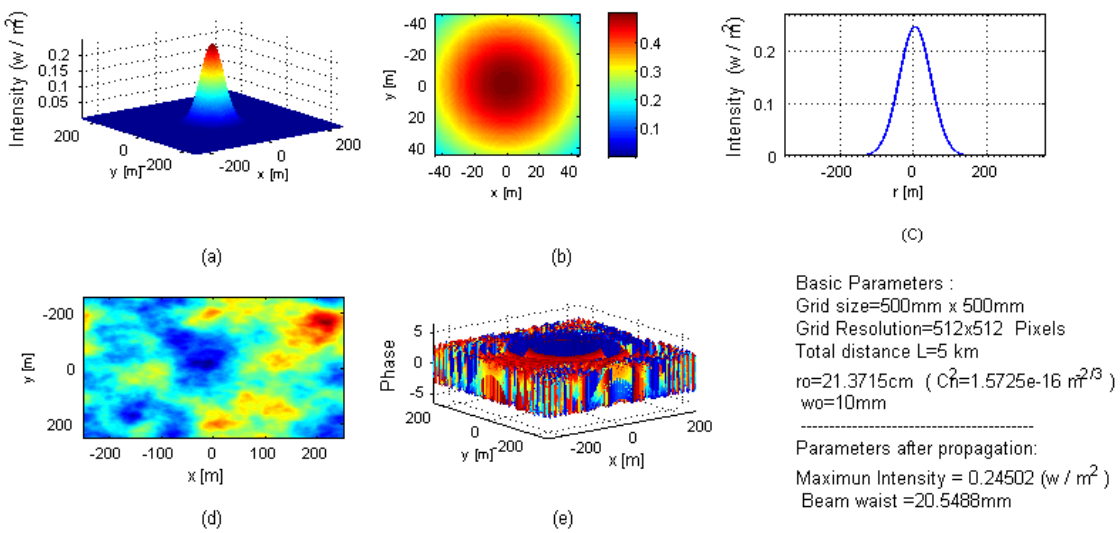

Fig.7. Gaussian beam propagation to distance z=L (phase screen at the object plane). (a) 3-D Gaussian beam, (b) Gaussian beam cross-section, (c) Gaussian beam profile, (d) Random phase screen profile, and (e) Gaussian beam phase distribution in transverse output plane.

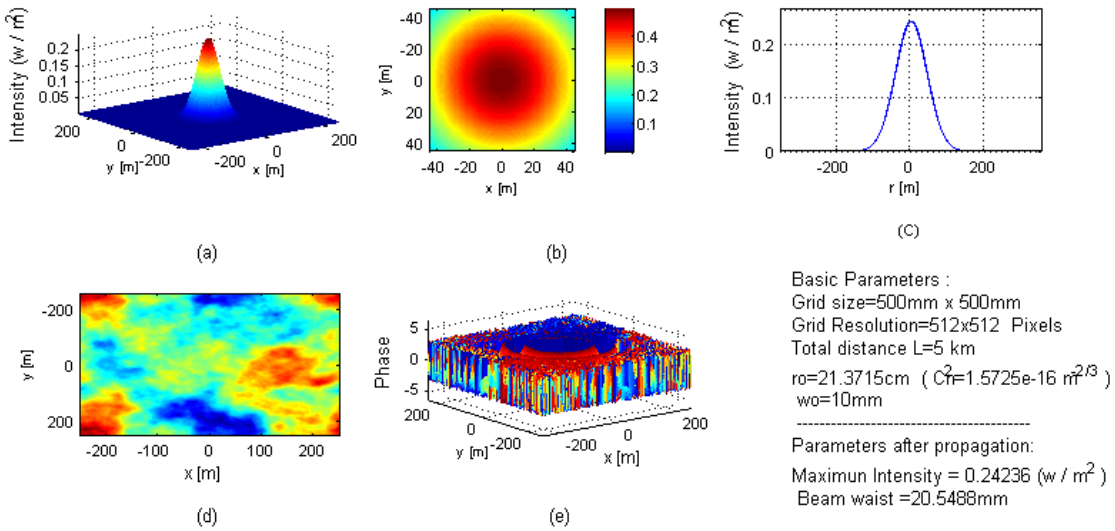

Fig.8. Gaussian beam propagation to distance z=L (phase screen at 0.5L). (a) 3-D Gaussian beam, (b) Gaussian beam cross-section, (c) Gaussian beam profile, (d) Random phase screen profile, and (e) Gaussian beam phase distribution in transverse output plane.

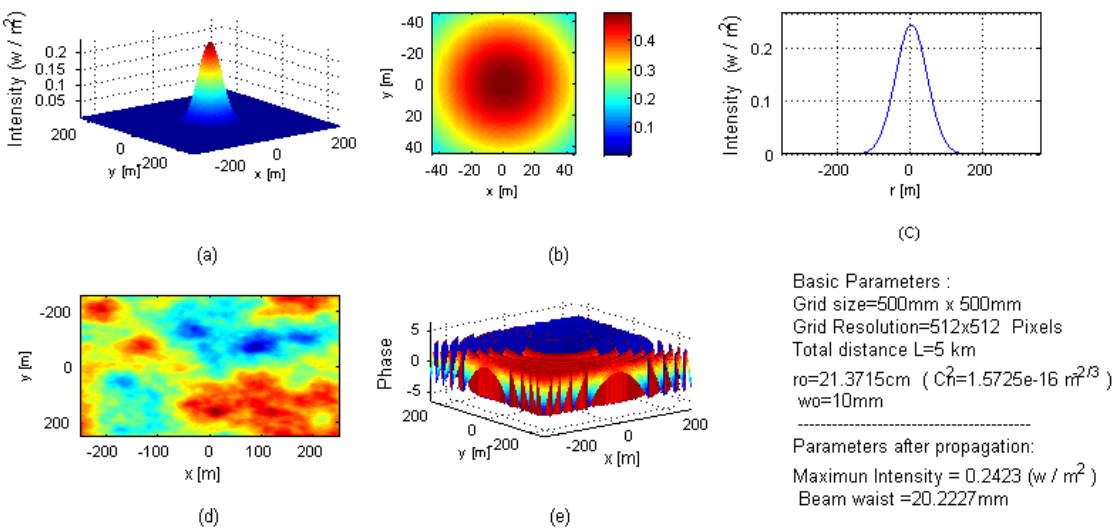

Fig.9. Gaussian beam propagation to distance z=L (phase screen at L or image plane). (a) 3-D Gaussian beam, (b) Gaussian beam cross-section, (c) Gaussian beam profile, (d) Random phase screen profile, and (e) Gaussian beam phase distribution in transverse output plane.

(b) Wide Gaussian beam (w0=100 mm)

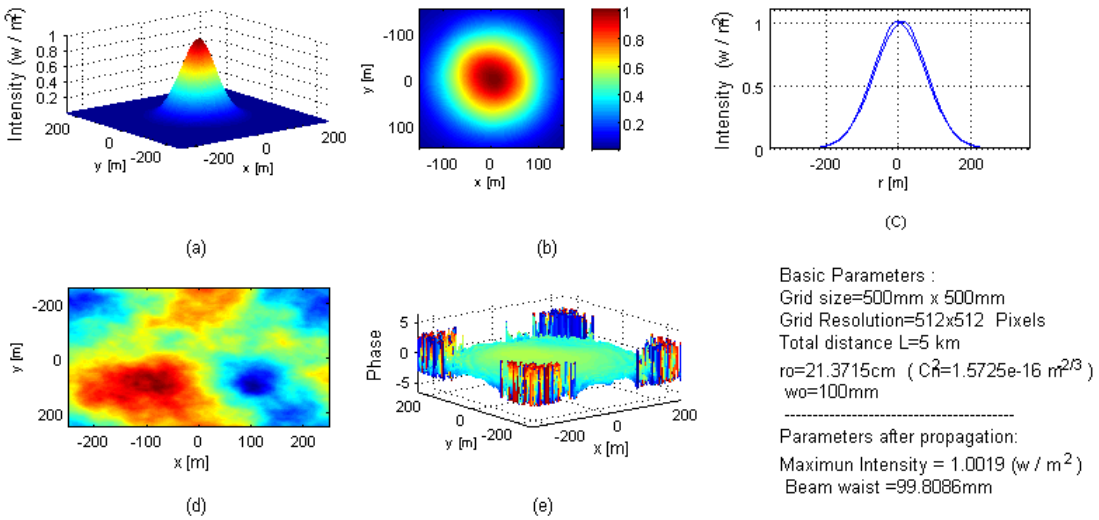

Fig.10. Gaussian beam propagation to distance z=L (phase screen at the object plane). (a) 3-D Gaussian beam, (b) Gaussian beam cross-section, (c) Gaussian beam profile, (d) Random phase screen profile, and (e) Gaussian beam phase distribution in transverse output plane.

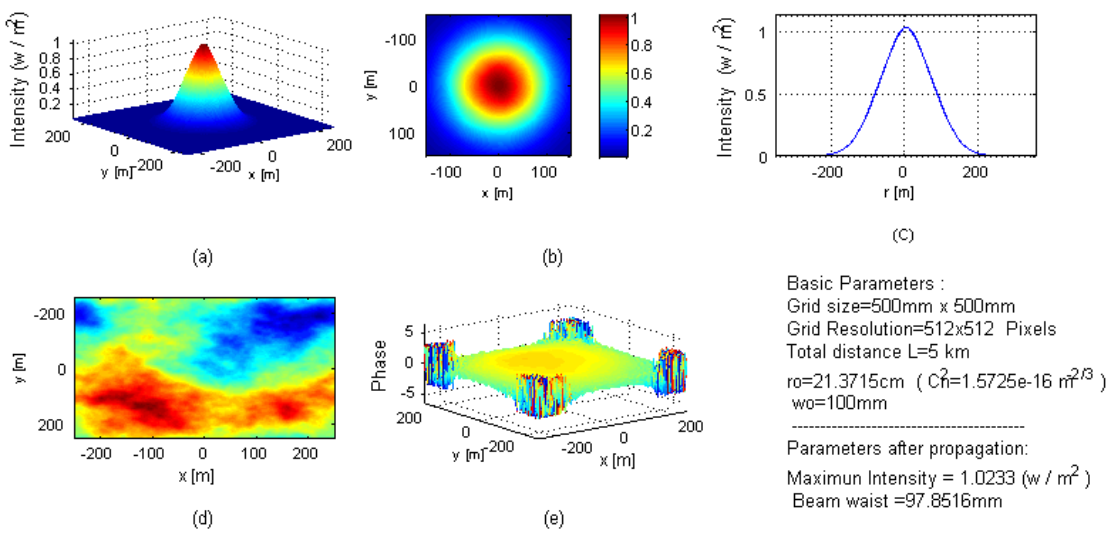

Fig.11. Gaussian beam propagation to distance z=L (phase screen at 0.5L). (a) 3-D Gaussian beam, (b) Gaussian beam cross-section, (c) Gaussian beam profile, (d) Random phase screen profile, and (e) Gaussian beam phase distribution in transverse output plane.

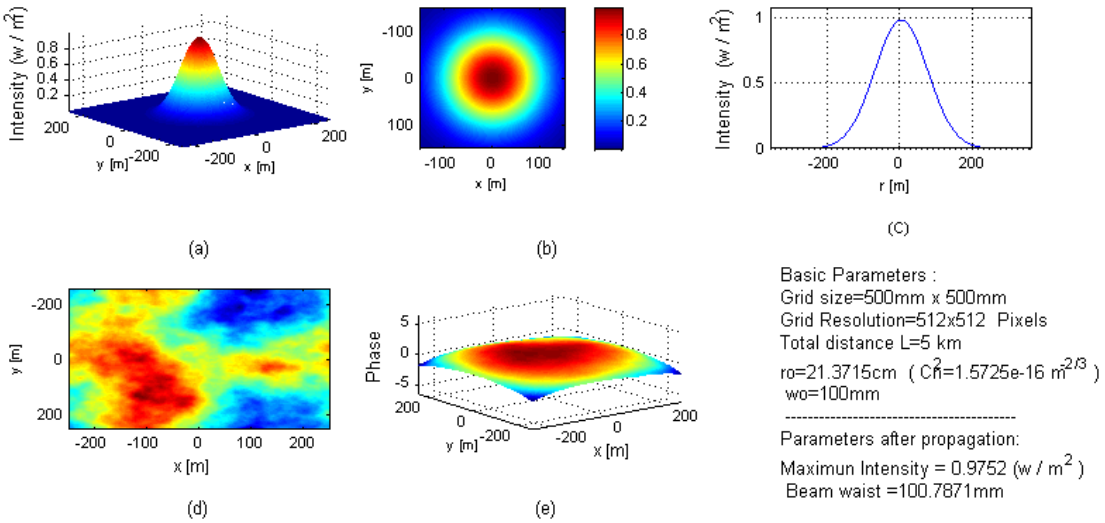

Fig.12. Gaussian beam propagation to distance z=L (phase screen at L or image plane). (a) 3-D Gaussian beam, (b) Gaussian beam cross-section, (c) Gaussian beam profile, (d) Random phase screen profile, and (e) Gaussian beam phase distribution in transverse output plane.

Figs.7-12 show that for narrow Gaussian beams under moderate turbulence, placement of the phase screen early in the propagation likely once again creates greater overall phase fluctuation profiles in the output beam. Additionally, there is possibly some beam amplitude splitting that happens at the output for early phase screen placements compared with placements further along the diffraction path. For wider Gaussian beams, similar amplitude-splitting behavior is once again evident; moreover, we also observe a phase "clustering" effect around the edges of the grid when the phase screen is placed well before the end of the propagation path. As before, there is also peak amplitude or intensity decay in the output beams. As mentioned before, further quantitative analyses of these phenomena are currently pending.

Case III. Propagation distance

In this case, we again consider moderate turbulence ($r_0 = 0.5$ mm or $C_n^2 = 7.8625 \times 10^{-16}$ $m^{-2/3}$).

For the cases studies presented here, the Fraunhofer or far-field distance (D^2/λ, where D is the grid size) happens to be about 250 km. Thus, all propagation cases reported herein apply only to *near-field* diffraction. In the report presented here, we simply discuss the effect of propagation distance upon the diffracted EM beam within the Fresnel regime, except that we compare relatively short versus longer longitudinal propagation distances.

(a) L=1km

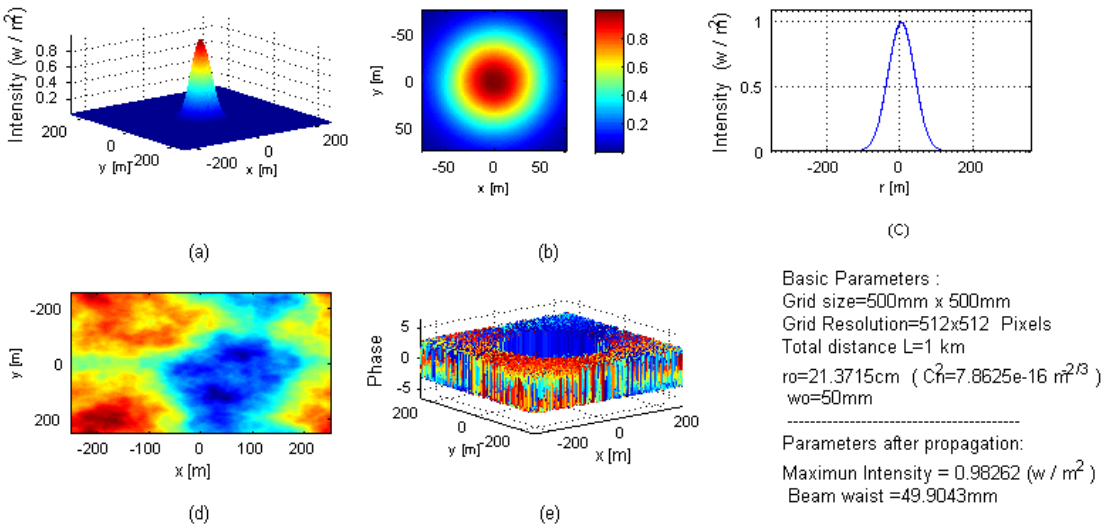

Fig.13. Gaussian beam propagation to distance z=L (phase screen at object plane). (a) 3-D Gaussian beam, (b) Gaussian beam cross-section, (c) Gaussian beam profile, (d) Random phase screen profile, and (e) Gaussian beam phase distribution in transverse output plane.

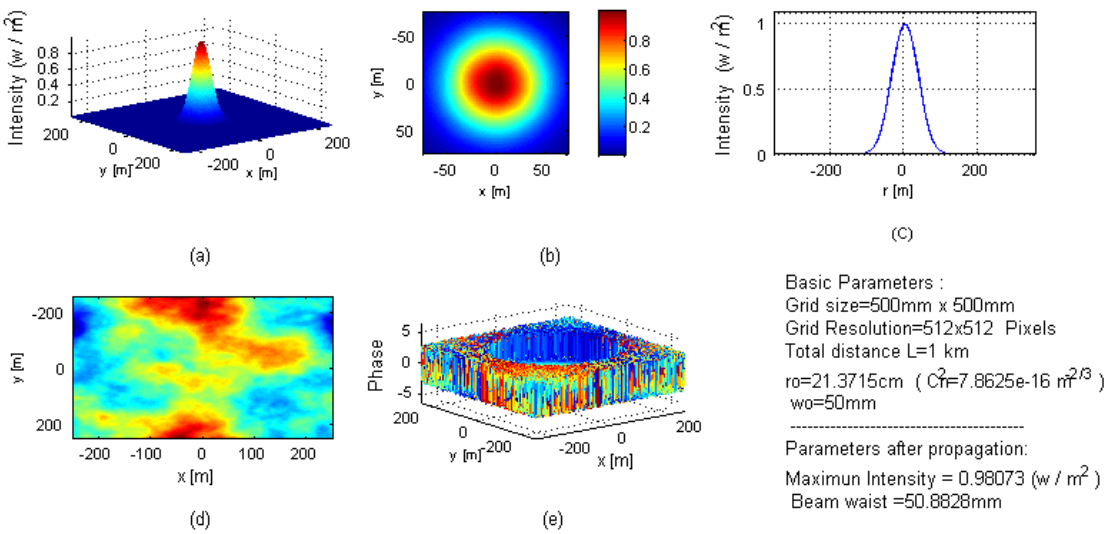

Fig.14. Gaussian beam propagation to distance z=L (phase screen at 0.5 L). (a) 3-D Gaussian beam, (b) Gaussian beam cross-section, (c) Gaussian beam profile, (d) Random phase screen profile, and (e) Gaussian beam phase distribution in transverse output plane.

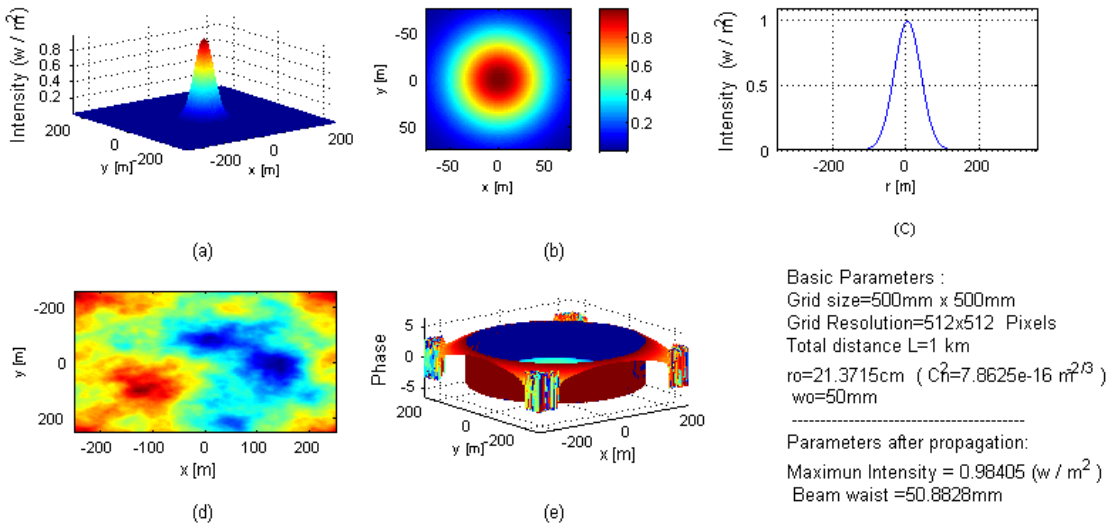

Fig.15. Gaussian beam propagation to distance z=L (phase screen at L or image plane). (a) 3-D Gaussian beam, (b) Gaussian beam cross-section, (c) Gaussian beam profile, (d) Random phase screen profile, and (e) Gaussian beam phase distribution in transverse output plane.

(b) L=10 km

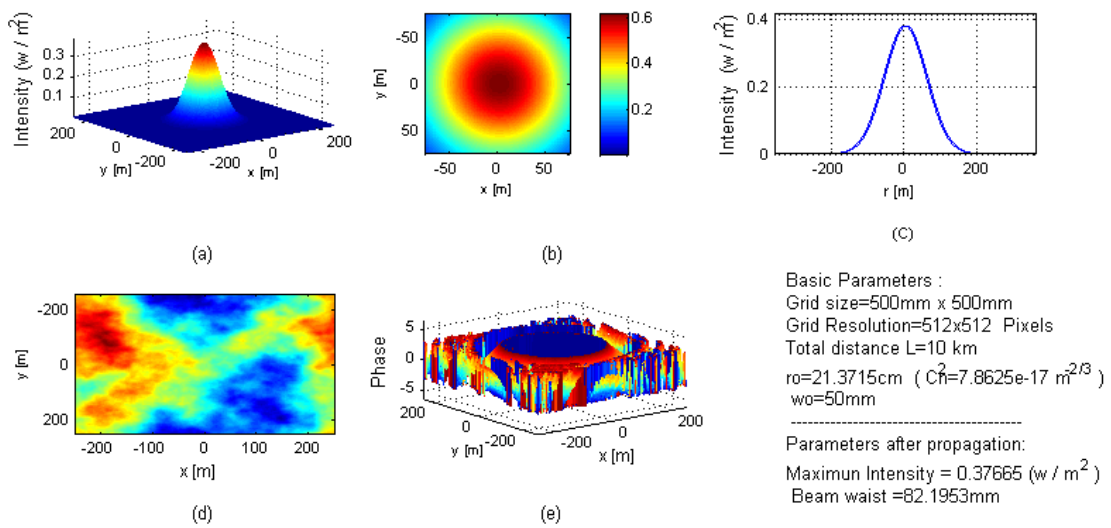

Fig.16. Gaussian beam propagation to distance z=L (phase screen at object plane). (a) 3-D Gaussian beam, (b) Gaussian beam cross-section, (c) Gaussian beam profile, (d) Random phase screen profile, and (e) Gaussian beam phase distribution in transverse output plane.

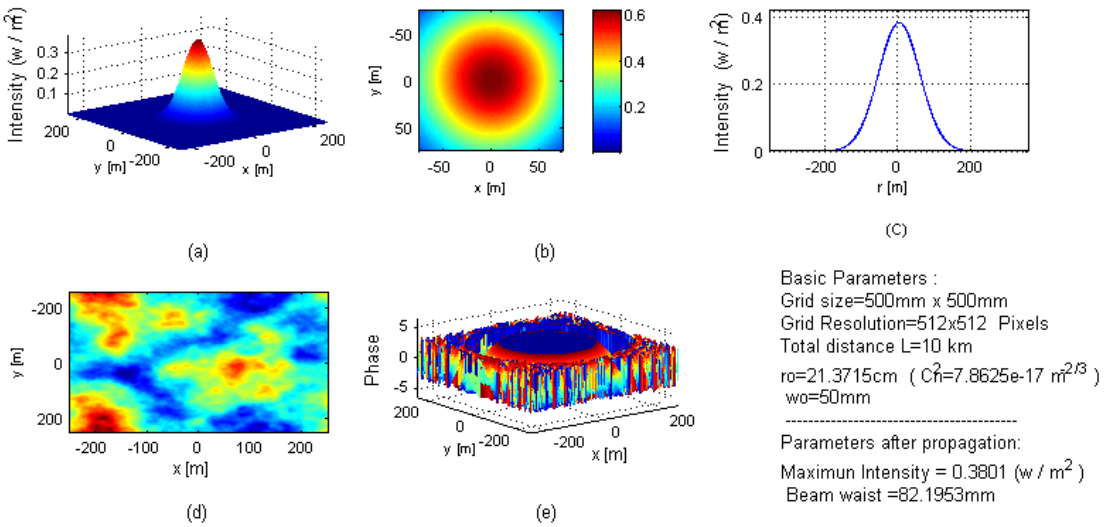

Fig.17. Gaussian beam propagation to distance z=L (phase screen at 0.5L or image plane). (a) 3-D Gaussian beam, (b) Gaussian beam cross-section, (c) Gaussian beam profile, (d) Random phase screen profile, and (e) Gaussian beam phase distribution in transverse output plane.

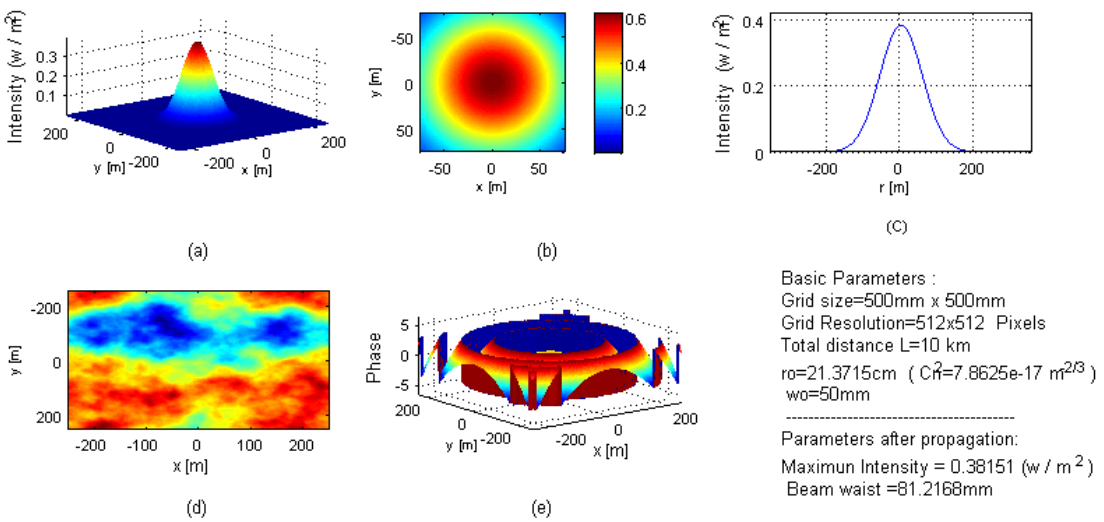

Fig.18. Gaussian beam propagation to distance z=L (phase screen at L or image plane). (a) 3-D Gaussian beam, (b) Gaussian beam cross-section, (c) Gaussian beam profile, (d) Random phase screen profile, and (e) Gaussian beam phase distribution in transverse output plane.

From Figs.13-18, we find that for propagation to shorter distances, the output EM beam suffers very little amplitude distortion or decay, and likely a small amount of diffractive broadening. On the other hand, the phase fluctuations are once again greater for earlier screen placements compared with placements later along the propagation path. For propagation to longer distances, we observe greater diffractive broadening, as expected. Additionally, there is also greater amplitude decay and greater phase fluctuation for earlier screen placement, as before. There is likely also a small amount of diffractive beam splitting in the output for early phase screen placement. Further quantitative analyses are also pending for this case.

4.2 Temporal statistics

We note at this stage that investigating the propagation of EM waves through atmospheric turbulence in the current work has been motivated by the problem of chaotic wave propagation through a turbulent layer. While the majority of turbulence models are in the spatial or inverse domains, the chaotic acousto-optic first-order light is characterized by time-dependent chaos. As a result, it becomes necessary to develop the means to track the turbulence as a function of time. One way to accomplish this is to realize that the random phase fluctuations associated with MVKS is also inherently a time-dependent phenomenon. Thus, the phase of an EM wave will not only fluctuate randomly in space (via inner and outer scales), but also with time. In the simulations presented here, this time fluctuation enter directly into the process because the random numbers used as part of the generation of the MVKS phase function will also automatically change randomly with time. Thus, one may evaluate temporal statistical measures of the output field in the system under study for both amplitude and phase in order to develop an appropriate temporal model. In this section, the temporal mean and variance of the amplitude and phase of the diffracted field are computed by placing the *single* random phase screen at arbitrary positions along the propagation path (say in steps of 0.1L from the object to the image planes) and evaluating the diffracted Gaussian beam at *image* plane (z=L). For each phase screen position, the *on-axis* mean and variance of the amplitude and phase of the field are calculated. A turbulence strength of $r_0 = 0.01$mm or $C_n^2 = 2.7 \times 10^{-13}$ $m^{-2/3}$, Gaussian beam waist of w_0=50mm, propagation distance L=5km, and number of sample points (grid resolution) 0f 513x513 are used for this computation. The number of samples (iterations) used to calculate the mean and variance of the amplitude and phase of the field is 500 times (N=500), i.e., the random phase screens across which the EM wave propagates are re-created 500 times. Fig.19 shows the mean and variance of the amplitude and phase of the diffracted Gaussian beam at z=L for different random phase screen positions.

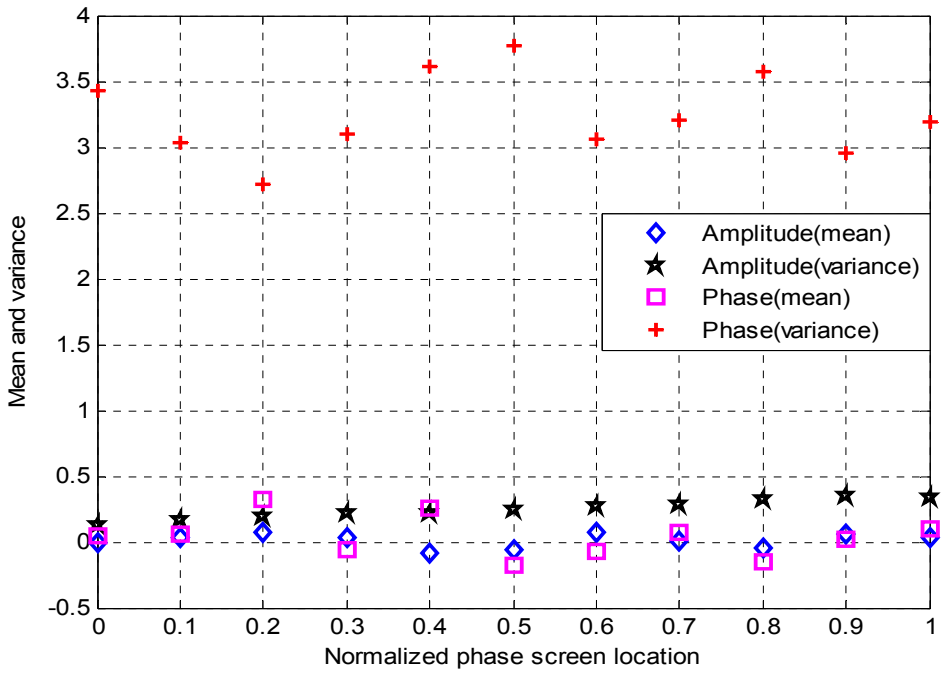

Fig.19. On-axis mean and variance of the amplitude and phase of diffracted Gaussian beam at Z=L for different random phase screen positions.

We note here that temporal statistics for points in the paraxial region as well as sufficiently off-axis have also been computed. Clearly, the overall scales of the time statistics in terms of corresponding inner and outer scales *in time* need to be examined and derived further. These and other relevant results will be analyzed and presented in follow-up work.

5. CONCLUDING REMARKS

In this work, we have studied the influence of atmospheric turbulence on profiled Gaussian beams propagating over distances in the 1 to 10 km range. A PSD of the MVKS was used to generate the random phase screen representing the random behavior of the turbulent atmosphere. Furthermore, a split-step propagation method involving Fresnel-Kirchhoff diffraction combined with transmission through a thin random phase screen was applied. Numerical simulations are presented for a narrow region of turbulence. Diffracted output fields are derived for different system parameters consisting turbulence strength, Gaussian beam waist and the propagation distance. The simulation results show that the diffracted Gaussian beam undergoes greater distortion for extended phase turbulence (results for this will be discussed elsewhere). Also, the Gaussian beam waist and the propagation distance are found to have a direct impact on the diffracted field under narrow atmospheric turbulence. Finally, on-axis temporal statistics (mean and variance) of the amplitude and phase of the diffracted Gaussian beam have been calculated in anticipation of the use of this information in tracking subsequent propagation of (modulated) chaotic waves through the turbulence. The goal would be to examine if a chaotic wave exhibits any degree of immunity relative to turbulence compared with deterministic, non-chaotic waves.

REFERENCES

[1] L. Sjöqvist, M. Henriksson and O. Steinvall, "Simulation of laser beam propagation over land and sea using phase screens – a comparison with experimental data," Proc. SPIE 5989, 59890-1-12 (2005).

[2] V.S. Rao Gudimetlaa, R.B. Holmesb, T.C. Farrella, and J. Lucas, "Phase screen simulations of laser propagation through non-Kolmogorov atmospheric turbulence," Proc. SPIE 8038, 803808-1-12 (May 2011).

[3] E.M. Whitfield, P.P. Banerjee and J.W. Haus, "Propagation of Gaussian beams through a modified von Karman phase screen," Proc. SPIE 8517,.85170-1-7 (Oct. 2012).

[4] L.C. Andrews, R.L. Phillips and A.R. Weeks, "Propagation of a Gaussian-beam wave through a random phase screen," *Waves in Random Media* 7, 229-244 (1997).

[5] X. Zhu and J.M. Kahn, "Free-space optical communication through atmospheric turbulence channels," IEEE Trans. Comm. 50, no. 8 (Aug. 2002).

[6] R.R. Kumar, A. Sampath and P. Indumathi, "Secure optical communication using chaos," Opt. Comm., Indian J. Science and Tech. 4, no. 7, 773-778, (July 2011).

[7] L. Larger and J. Goedgebuer, "Encryption using chaotic dynamics for optical telecommunications," C. R. Physique 5,. 609–611 (2004).

[8] M. R. Chatterjee and M. Alsaedi, "Examination of chaotic signal encryption and recovery for secure communication using hybrid acousto-optic feedback" Opt. Eng. 50, no. 5, 055002-1- 14 (May 2011).

[9] J. D. Schmidt, *Numerical Simulation of Optical Wave Propagation with Examples in Matlab*, SPIE Press: Bellingham, WA (2010).

[10] T. C. Poon and T.Kim, *Engineering Optics with Matlab*, World Scientific: Singapore (2006).

[11] L.C. Andrews and R.L. Phillips, *Laser Beam Propagation through Random Medium*, 2nd Ed., SPIE Press: Bellingham, WA (1998).

[12] M.C. Roggemann and B.M Welsh, *Imaging Through Turbulence*, CRC Press: Boca Raton, FL (1996).